VISCOUS DISSIPATION ON BIOCONVECTION FLOW OF WALTER-B NANOFLUID OVER A STRETCHING SURFACE WITH ACTIVATION ENERGY

by

Ibrahim MAHARIQ [a,b,c,d], ***Shiraz AHMAD*** [e], ***Saeed ISLAM*** [f*], ***Ishtiaq ALI*** [g], ***Irfan MUSTAFA*** [e], ***Hakeem ULLAH*** [h*], ***and Ali AKGUL*** [i,j,k,l*]

[a] Najjad Zeenni Faculty of Engineering, Al-Quds University, Jerusalem, Palestine
[b] University College, Korea University, Seoul, South Korea
[c] Department of Medical Research, China Medical University Hospital, China Medical University, Taichung, Taiwan
[d] Applied Science Research Center, Applied Science Private University, Amman, Jordan
[e] Department of Mathematics, Allama Iqbal Open University, Islamabad
[f] Department of Mechanical Engineering, Prince Mohammad Bin Fahd University, Al Khobar, Saudi Arabia
[g] Department of Mathematics and Statitics, College of Science, King Faisal University, Al-Ahsa, Saudi Arabia
[h] Department of Mathematics, Abdul Wali Khan University, Mardan, Khyber Pakhtunkhwa, Pakistan
[i] Department of Electronics and Communication Engineering, Saveetha School of Engineering, SIMATS, Chennai, Tamilnadu, India
[j] Siirt University, Art and Science Faculty, Department of Mathematics, Siirt, Turkey
[k] Applied Science Research Center, Applied Science Private University, Amman, Jordan
[l] Department of Computer Engineering, Biruni University,Topkapı, Istanbul, Turkey

Original scientific paper
https://doi.org/10.2298/TSCI2504167M

This study examines how bioconvection is affected by viscous dissipation in Walter-B nanofluid-flow across a stretching surface while taking activation energy into account. There are several uses for viscous dissipation in many different domains. These applications span from comprehending natural phenomena to engineering and manufacturing processes. Which include material processing methods like polymer extrusion, fluid-flow optimization in high speed applications, and heat transfer augmentation in various systems. A mathematical model is developed by using stress tensor of Walter-B fluid model and Buongiorns model to analyze the dynamics of nanofluid. The only two slip mechanism namely thermophoretic and Brownian motion are discussed. Using the shooting technique bvp4c, to address the non-linear ODE. The following factors are examined: radioactivity, magnetic parameter, Soret number, Peclet number, Brownian motion parameter, Prandtl number, Dufour number, Lewis number for bioconvection, radiation parameter, and melting parameter. A graphic representation of the effects of the pertinent factors on the velocity, temperature, and concentration profiles are shown, together with the Sherwood number, Nusselt number, and skin friction coefficient. With a rise in the magnetic and viscoelastic parameters, velocity decreases. The temperature upsurges with increases in the radiation parameter, magnetic parameter, Dufour number, and Brownian motion parameter. The concentration rises with an in-

* Corresponding authors, e-mail: sislam@pmu.edu.sa; hakeemullah1@gmail.com; aliakgul00727@gmail.com

crease in the thermophoresis parameter, but falls with an increase in the Brownian motion parameter. As the Peclet number and Bioconvection Lewis number rise, so does the field of microorganisms.

Key words: *Walter-B nanofluid, bioconvection, viscous dissipation, activation energy, thermophoresis, Brownian motion*

Introduction

Walter B liquid, a subclass of non-Newtonian liquids, is used in many industrial domains, including as chemical research, biosystems, chemical manufacturing, bioengineering, and biophysical techniques of thermal conduction in tissues. It was Walter who created the Walter-B liquid connection [1]. Nandeppanavar *et al.* [2] looked at the effects of nanomaterials on Walter-B liquid. A sort of synthetic fluid known as *nanofluid* is one in which nanoparticles-particles smaller than 100 nanometers are uniformly dispersed throughout a base fluid, including water, oil, or ethylene glycol. These fluids are made to have greater thermal and physical characteristics than the base fluid alone, including increased thermal conductivity, better heat transfer, and improved stability. Nanofluids are frequently utilized in innovative energy technologies, heat exchangers, and cooling systems because of their exceptional performance in heat and mass transfer processes. Choi and Eastman [3] was the first to propose the concept of highly sophisticated fluids. Buongiorno [4] introduced the mathematical model for these sophisticated fluids' conveyance. Hayat *et al.* [5] investigated the effects of non-linear radiation and activation energy in mixed convective hydrodynamics. The Jeffrey nanomaterial flows when the cylinder is extended. We examined the importance of Brownian motion and thermophoresis. The heat transfer phenomenon generated by nanofluid with joule heating application was investigated by Asghar *et al.* [6]. A moving curved surface was employed by Nadeem *et al.* [7] to investigate the diverse heat pattern associated with the hybrid nanofluid. Eshgarf *et al.* [8] articulate the single-phase nanofluid analysis through a thorough review. The function of nanoparticles in channel flow with thermofluidic transport was examined by Ali *et al.* [9]. The Sutter by nanofluid against 3-D flow was the main focus of Azam *et al.* [10]. Hussain and Sheremet [11] used the porous region help the nanofluid move convectively. Using a declining surface, Acharya and Kalidas [12] predicted the entropy production analysis for nanofluid. Using the nanofluid model, Sharma *et al.* [13] demonstrated improved characteristics of blood-based micropolar liquids. Moatimid *et al.* [14] investigated the thermal consequences of the Reiner-Rivlin nanofluids contact with a stretched disk. Turkyilmazoglu [15] examined the movement of nanomaterials on vertical surfaces. Muhammad *et al.* [16] investigated 3-D radiative Eyring-Powell nanoliquid transfer with activation energy using a Riga plate. Anwan *et al.* [17] observed non-linear radiative heat transmission using MHD nanoliquid spray.

Heat is created when a fluid's viscosity resists motion and gradients transform its kinetic energy into internal energy (heat). This process is known as viscous dissipation. Viscous dissipation effects are important in supersonic and hypersonic vehicle design because of the high velocities and sharp velocity gradients close to the surface. Viscosity dissipation is crucial in micro-fluidic devices because of the tiny scale and large velocity gradients. It is also a crucial consideration in the design of bearings and lubricants. Energy losses and efficiency in turbines, compressors, and pumps are impacted by viscous dissipation. Validating CFD models for thermal analysis is another important function of it. Sheikholeslami *et al.* [18] used the zigzag motion impacts of nanoparticles on MHD nanofluid-flow between two plates in a rotating system to explain the effects of viscous dissipation and introduce the fluid problem. They discovered

that there is an inverse relationship between the dissipation parameter and the heat transfer rate. Maleki *et al.* [19] talked about how well a pseudo-plastic nanofluid performed as it passed a moveable porous surface with a dissipation effect. Saleem *et al.* [20] investigated fluid-flow in nanomaterials under the impact of viscous dissipation. By using the optimal homotopy analysis technique, they were able to construct an analytical solution and demonstrate how the dissipation parameter improves the temperature fieldby include heat generation and absorption, Ganga *et al.* [21] examined the effects of viscous-ohmic [J] heating on MHD nanofluid-flow approaching a plate. Their findings indicate that the magnetic and dissipation characteristics cause the rate of heat transmission decrease.

A boundary or surface that experiences continuous deformation from stretching in a fluid or solid medium is referred to as a stretching surface. This is a typical occurrence in fluid dynamics, thermodynamics, and materials science, when forces drive a surface (such as a flat plate or sheet) to stretch or expand in one or more directions. In addition their practical uses in engineering, technology, and environmental sciences, the Navier-Stoke equations for fluid-flow and energy and the diffusion equations for heat and mass transfer are frequently employed in mathematical modelling of stretched surfaces. During the extrusion process, it is crucial to examine the fluid motion brought on by the stretching surface. Crane [22] solved the problem of steady 2-D flow by first extending boundaries. Similar solutions to the boundary-layer equations describing the unsteady flow and heat transport across an irregular stretched sheet have been provided by Elbashbeshy and Bazid [23]. Sharidan *et al.* [24] investigated heat transfer and unsteady flow across a stretching sheet in a viscous and incompressible fluid. Tsai *et al.* [25] also found similar solutions for unsteady flow and heat transfer across an extending sheet under different conditions [26]. Hayat and Awais [27] investigated the flow over a elongating surface in relation time. The effect of slip on unstable boundary-layer stagnation point flow across a stretching sheet was examined by Bhattacharyya *et al.* [28]. The 3-D flow of Jeffery fluid past a stretched surface was also covered by Hayat *et al.* [29].

In 1889, a scientist named Svante Arrhenius coined the term *energy activation*. According to him, energy activation is the amount of energy required to overcome an organic compound's chemical reaction. Additionally, it focused on the minimum amount of energy needed to start chemicalreaction. In the combination of heat and mass transport, it is crucial. Additionally, materials for batteries, fuel, cells, and semiconductors are optimized using it. Rashid *et al.* [30] examined how activation energy behaved in Maxwell nanoliquid MHD flow. The MHD heat-transport of nanoliquids when wave conduction rings generated was examined by Tayebi *et al.* [31]. The activation energy of third-grade MHD nanoliquid-flow wasdiscussed by Hayat *et al.* [32]. Dawar *et al.* [33] conducted a magnetic field flow of a nanoliquid containing activation energy. A few relevant works are listed in Refs. [33-40].

In this paper, we extend the analysis of [41] in four key directions:

– Incorporate the presence of nanoparticles into the flow model, with focus on Brownian motion and thermophoretic diffusion.
– Introduce the influence of Arrhenius activation function in the concentration equation.
– The influence of the swimming gyrotactic motile microorganisms.
– For the solution of the non-linear equation bvp4c technique in MATLAB software is used.

The consequences of different flow parameters are presented graphically and discussed in detail.

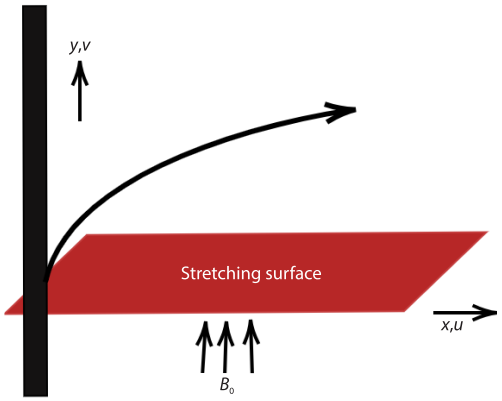

Figure 1. Geometry of the flow

Problem formulation

The bioconvection Walter-B nanofluid 2-D flow caused by the stretching surface investigated in the present model. The Cartesian co-ordinates (x, y) are chosen with velocities u and v, respectively, fig. 1. A uniform magnetic field, B_0, is applied parallel to the y-axis. Brownian motion and thermophoretic diffusion are taken into consideration. Furthermore, the presence of gyrotactic microorganisms is examined in relation the Dufour and Soret effects. Assume that the flow is due to the stretching of the sheet along x-axis with velocity $u_w = ax$ where $a > 0$ is constant. Using the aforementioned assumption the governing flow equations are [41]:

$$\frac{\partial u}{\partial x}+\frac{\partial v}{\partial y}=0 \tag{1}$$

$$u\frac{\partial u}{\partial x}+v\frac{\partial u}{\partial y}=\frac{\mu}{\rho_{\mathrm{f}}}\frac{\partial^2 u}{\partial y^2}-\frac{k_0}{\rho_{\mathrm{f}}}\left(u\frac{\partial^3 u}{\partial x\partial y^2}+v\frac{\partial^3 u}{\partial y^3}-\frac{\partial u\partial^2 u}{\partial y\partial x\partial y}+\frac{\partial u\partial^2 u}{\partial x\partial y^2}\right)-\frac{\sigma B_0^2}{\rho_{\mathrm{f}}}u \tag{2}$$

$$\begin{aligned}u\frac{\partial T}{\partial x}+v\frac{\partial T}{\partial y}=&\frac{k}{(\rho c_p)_{\mathrm{f}}}\frac{\partial^2 T}{\partial y^2}+\frac{16\sigma^* T_\infty^3\partial^2 T}{3k^*\left(\rho c_p\right)_{\mathrm{f}}\partial y^2}+\tau\left[D_B\frac{\partial C\partial T}{\partial y\partial y}+\frac{D_T}{T_\infty}\left(\frac{\partial T}{\partial y}\right)^2\right]+\\&+\frac{D_B k_T\partial^2 C}{c_p c_s\partial y^2}+\frac{\sigma B_0^2}{(\rho c_p)_{\mathrm{f}}}u^2+\frac{\mu}{\rho_{\mathrm{f}}}\left(\frac{\partial u}{\partial y}\right)^2+\frac{\theta(T-T_m)}{\left(\rho c_p\right)_{\mathrm{f}}}\end{aligned} \tag{3}$$

$$u\frac{\partial C}{\partial x}+v\frac{\partial C}{\partial y}=\frac{D_T}{T_\infty}\frac{\partial^2 T}{\partial y^2}+D_B\left(\frac{\partial^2 C}{\partial y^2}\right)+\frac{D_B k_T\partial^2 T}{T_m\partial y^2}+kr^2(C-C_\infty)\left(\frac{T}{T_\infty}\right)^n\exp\left(-\frac{Ea}{k_a T}\right) \tag{4}$$

$$u\frac{\partial N}{\partial x}+v\frac{\partial N}{\partial y}=D_m\frac{\partial^2 N}{\partial y^2}-\frac{bW_c}{C_\infty-C_m}\left[\frac{\partial}{\partial y}\left(N\frac{\partial C}{\partial y}\right)\right] \tag{5}$$

With boundary constraints:

$$\begin{aligned}&u=ax,\ T=T_w,\ N=N_w,\ C=C_w,\ v=0\ \text{ at }\ y=0,\\&u\to 0,\ T\to T_\infty,\ N\to N_\infty, C\to C_\infty\ \text{ as }\ y\to\infty\\&k\left(\frac{\partial T}{\partial y}\right)_{y=0}=\rho_{\mathrm{f}}\left[\lambda^*+c_s(T_m-T_0)\right]v(x,0)\end{aligned} \tag{6}$$

where B_0 is the express magnetic field strength, D_B – the Brownian motion coefficien, μ – the dynamic viscosity, σ^* – the Stephan-Boltzmann constan, c_s – the heat capacity, λ^* – the latent heat, b – the chemotoxis constant, D_T – the thermophoretic diffusion coeffcients, D_m – the microorganisms diffusion coefficient, W_c – the swimming cell speed, C – the concentration of nanoparticles, N – the microorganisms concentration, ρ – the fluid density, T – the temperature, k – the thermal conductivity, T_m – the surface temperature, c_p – the nanoparticles concentration at surface, N_∞ – the ambient microorganisms concentration, and N_w – the microorganisms surface concentration, respectively.

For thermophysical properties of the nanoparticle-water nanofluid, the equations are defined for the effective density:

$$\rho_{\mathrm{nf}} = (1-\phi)\rho_b + \phi\rho_p \tag{7}$$

where ρ_{b} and ρ_{p} are the density base fluid and nanoparticles, respectively, and ϕ is the nanoparticle volume fraction.

Dynamic viscosity:

$$\mu_{\mathrm{nf}} = \frac{\mu_{\mathrm{b}}}{(1-\phi)^{2.5}} \tag{8}$$

where μ_{nf} and μ_{b} are the viscosity of the nanofluid and base fluid.

Heat capacity.

$$(\rho C_p)_{\mathrm{nf}} = \phi(\rho C_p)_{\mathrm{p}} + (1-\phi)(\rho C_p)_{\mathrm{b}} \tag{9}$$

Thermal conductivity :

$$k_{\mathrm{nf}} = \frac{k_{\mathrm{p}} + 2k_{\mathrm{b}} - 2\phi(k_{\mathrm{b}} - k_{\mathrm{p}})}{k_{\mathrm{p}} + 2k_{\mathrm{b}} + \phi(k_{\mathrm{b}} - k_{\mathrm{p}})} \tag{10}$$

where k_{nf} and k_{b} are the thermal conductivity of nanofluid and base fluid and k_{p} is the thermal conductivity of the particle. The Cartesian co-ordinates (x, y) are chosen with velocities u and v respectively, fig. 1.

Table 1. The physical properties of water and nanofluid

Base fluid and nanoparticle	ρ [kgm^{-3}]	C_p [Jkg^{-1}K^{-1}]	k [Wm^{-1}K^{-1}]	σ [Ω^{-1}m^{-1}]
Water	997.1	4179	0.613	0.005
Al_2O_3	3970	765	40	$35\cdot10^7$

Consider similarities transformations are used to change the PDE to ODE:

$$\begin{gathered} u = axf'(\eta),\ v = -\sqrt{av}f(\eta),\ \eta = \sqrt{\frac{a}{v}}y \\ \chi(\eta) = \frac{N - N_\infty}{N_w - N_\infty},\ \phi(\eta) = \frac{C - C_\infty}{C_w - C_\infty},\ \theta(\eta) = \frac{T - T_\infty}{T_w - T_\infty} \end{gathered} \tag{11}$$

After utilizing eq. (7), the non-dimensional form of the ODE are obtained:

$$f'''(\eta) + f(\eta)f''(\eta) - f'^2(\eta) + \beta\left[f''^2(\eta) - 2f'(\eta)f'''(\eta) + f(\eta)f''''(\eta)\right] - Mf'(\eta) = 0 \tag{12}$$

$$\begin{gathered} (1+Rd)\theta''(\eta) + \mathrm{Pr}\, f(\eta)\theta'(\eta) + \mathrm{Pr}\, Nb\theta'(\eta)\phi'(\eta) + \mathrm{Pr}\, Nt\theta'^2(\eta) + \mathrm{Pr}\,\mathrm{Du}\phi''(\eta) + \\ + M\mathrm{Br}f'^2(\eta) + \mathrm{Br}f''^2(\eta) + \mathrm{Pr}\, Q(\theta(\eta)) = 0 \end{gathered} \tag{13}$$

$$\phi''(\eta) + \frac{Nt}{Nb}\theta''(\eta) + \mathrm{Sc}f(\eta)\phi'(\eta) + \mathrm{ScSr}\theta''(\eta) + \sigma^*\phi(\eta)(\theta(\eta)\delta_0 + 1)^n \exp\left(-\frac{E}{\theta(\eta)\delta_0 + 1}\right) = 0 \tag{14}$$

$$\chi''(\eta) + \mathrm{Lb}f(\eta)\chi'(\eta) - \mathrm{Pe}\left[\phi''(\eta)(\chi(\eta) + \Omega) + \phi'(\eta)\chi'(\eta)\right] = 0 \tag{15}$$

The associated transformed boundary conditions are:

$$\begin{gathered} f'(0) = 1,\ f'(\infty) = 0,\ \theta(\infty) = 0,\ \phi(0) = 1,\ \theta(0) = 1 \\ \mathrm{Pr}\, f(0) + Me\theta'(0) = 0,\ \phi(\infty) = 0,\ \chi(0) = 1,\ \chi(\infty) = 0 \end{gathered} \tag{16}$$

where

$\delta_0 = \dfrac{T_m - T_\infty}{T_\infty}$ is the temperature difference number, $E = \dfrac{Ea}{k_a T_\infty}$ is the activation energy number,

$\mathrm{Sr} = \dfrac{D_B K_T (T_\infty - T_m)}{\nu T_\infty (C_\infty - C_m)}$ is the Soret number, $M = \dfrac{\sigma B_0^2}{\rho a}$ is the magnetic parameter,

$\mathrm{Pr} = \dfrac{\mu c_p}{k}$ is the Prandtl number, $\mathrm{Sc} = \dfrac{\nu}{D_B}$ is the Schmidt number,

$Nt = \dfrac{\tau D_T (C_\infty - C_m)}{\nu}$ is the thermophorosis parameter,

$\Omega = \dfrac{Nm}{N_\infty - N_m}$ is the microoraganisms concentration difference,

$Lb = \dfrac{\nu}{D_B}$ is the bioconvection Lewis number,

$Nb = \dfrac{\tau D_B (C_\infty - C_m)}{\nu}$ is the Brownian motion parameter,

$\mathrm{Rd} = \dfrac{16\sigma^* T_\infty^3}{3kk^*}$ is the radiation parameter, $\mathrm{Pe} = \dfrac{bW_c}{D_n}$ is the Peclet number, and

$Me = \dfrac{c_p (T_\infty - T_m)}{\lambda^* + c_s (T_m - T_0)}$ is the melting variable, respectively.

Solution methodology

Now let us we have:

$$y = f,\ y_1 = f',\ y_2 = f'',\ y_3 = f''',\ y_3' = f^{iv},\ y_4 = \theta,\ y_5 = \theta',\ y_5' = \theta'',\ y_6 = \phi,\ y_7 = \phi',\ y_7' = \phi'',\ y_8 = \chi,\ y_8 = \chi' \tag{17}$$

Then the momentum, energy, nanoparticles, and microorganisms equations becomes:

$$y_3' = \frac{y_3 - y y_2 + y_1 y_1 - \beta\left(y_3 y_3 - 2 y_2 y_3\right) + M y_1}{\beta y} \tag{18}$$

$$y_5' = \frac{-\mathrm{Pr}\, y y_5 - \mathrm{Pr}\,\mathrm{Br} y_1 y_1 - \mathrm{Br} y_2 y_2 - \mathrm{Pr}\left(Nb y_5 y_7 + Nt 2 y_5 y_5\right) - \mathrm{Pr}\, Q y_4 - \mathrm{Pr}\, Bu y_7'}{1 + Rd} \tag{19}$$

$$y_7' = -\mathrm{Sc} y y_7 - \frac{Nt}{Nb} y_5' - Br y_2 y_2 - \mathrm{ScSr} y_5' - \mathrm{Sc}\sigma^* \left(1 + \delta_0 y_4\right)^n \exp\left[\frac{-E}{1 + \delta_0 y_4}\right] \tag{20}$$

$$y_9' = -Lb y y_9 - \frac{Nt}{Nb} y_5' + \mathrm{Pe}\left[y_7'\left(y_8 + \Omega\right) + y_9 y_7\right] \tag{21}$$

Boundary conditions are:

$$y_{1a} - 1,\ y_{1b} - 0,\ y_{4a} - 0, y_{6a} - 1,\ y_{4b} - 1,\ \mathrm{Pr}\, y_a + Me y_{5a} - 0,\ y_{6b} - 0, y_{8a} - 1,\ y_{8b} - 0 \tag{22}$$

Results discussion

The behavior of several factors on velocity, temperature distribution, nanoparticle concentration, and microbe concentration is displayed in this section.

Figure 2 shows how the viscoelastic parameter affects, $f'(\eta)$. The fluid velocity drops as, β, increases, resulting in a thinner thickness of the momentum barrier layer. The boundary-layer contracts due to the tensile stress caused by the viscoelasticity, which lowers velocity. Figure 3 illustrates how the porosity parameter, *kp*, affects the velocity profile. Higher *kp* values indicate a declining velocity profile. This is because a rise in *kp* thickens the boundary-layer by increasing the fluid resistance across the surface. Figure 4 illustrates the effect of the magnetic parameter, demonstrating how the velocity field varies as the magnetic parameter rises. As the magnetic parameter value rises, velocity falls. Increased magnetic field strength creates Lorentz forces, which increase flow resistance and cause velocity to decrease. Figure 5 illustrates how the melting parameter affects the velocity profile, demonstrating that a higher melting param-

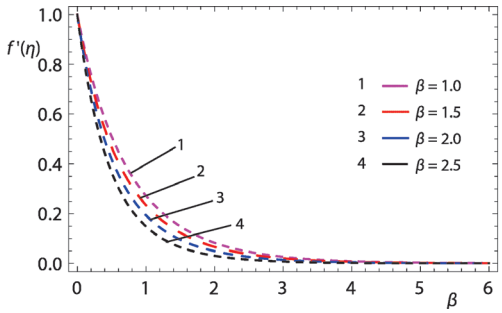

Figure 2. The $f'(\eta)$ *vs.* viscoelastic parameter, β

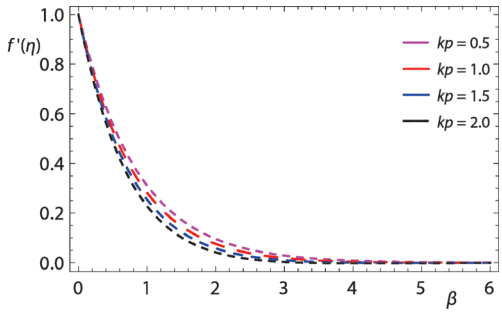

Figure 3. The $f'(\eta)$ *vs.* porosity parameter, *kp*

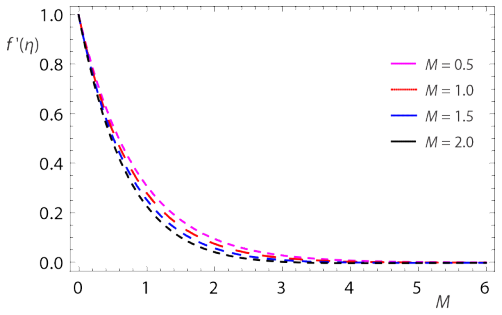

Figure 4. The $f'(\eta)$ *vs.* magnetic parameter, *M*

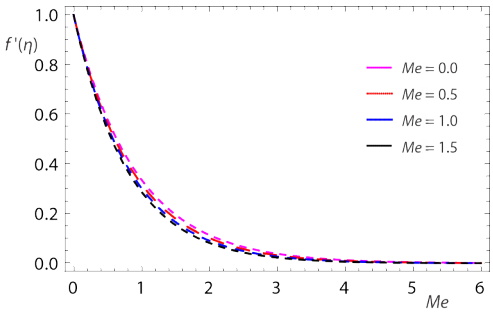

Figure 5. The $f'(\eta)$ *vs.* melting parameter, *Me*

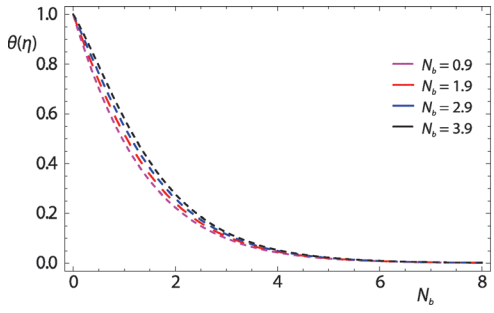

Figure 6. The $\theta(\eta)$ *vs.* Brownian motion parameter, *Nb*

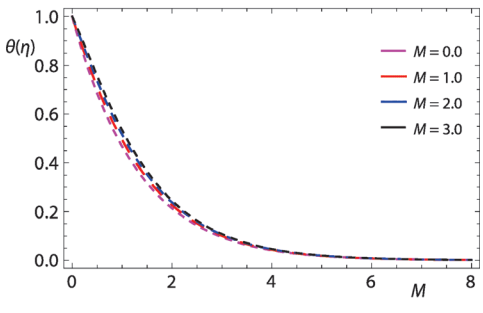

Figure 7. The $\theta(\eta)$ *vs.* magnetic parameter, *M*

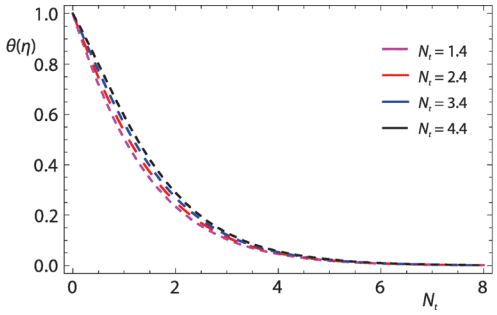

Figure 8. The $\theta(\eta)$ *vs.* thermophoresis parameter, *Nt*

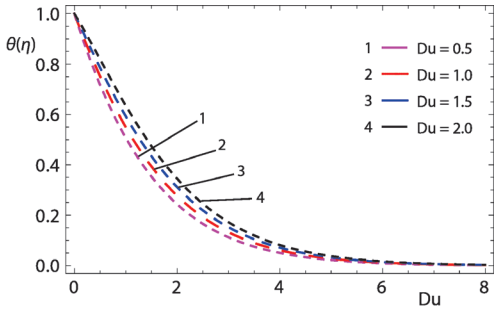

Figure 9. The $\theta(\eta)$ *vs.* Dufour number

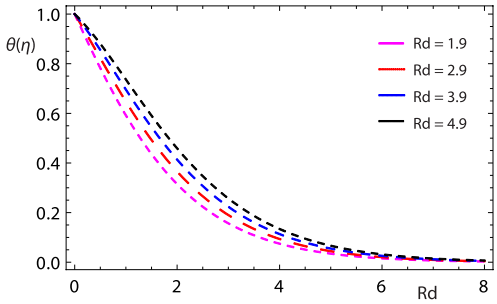

Figure 10. The $\theta(\eta)$ *vs.* radiation parameter, *Rd*

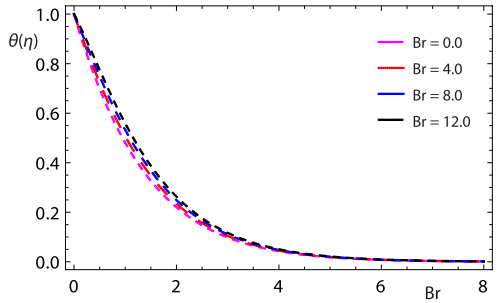

Figure 11. The $\theta(\eta)$ *vs.* Brinkman number

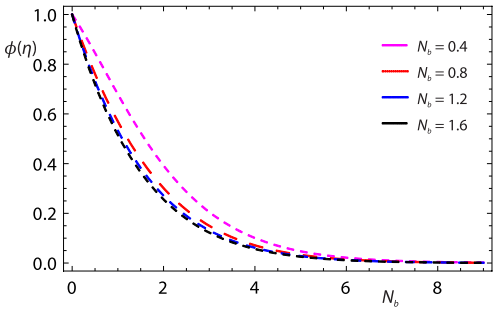

Figure 12. The $\phi(\eta)$ *vs.* Brownian motion parameter, *Nb*

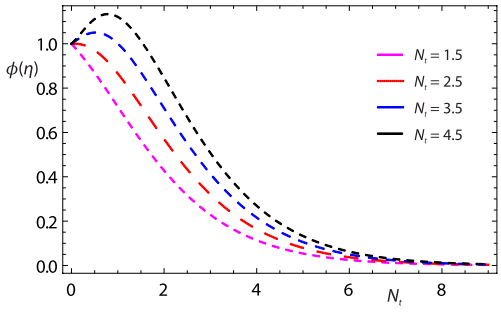

Figure 13. The $\phi(\eta)$ *vs.* thermophoresis parameter, *Nt*

eter results in a lower velocity profileindicating that when more heat is absorbed as a result of the melting process, fluid momentum decreases and velocity subsequently decreases, slowing down fluid-flow. The effect of *Nb*, in temperature profile as seen in fig. 6, a measurement of the nanoparticles' random motion, raises the temperature close to the boundary-layer. Physically, the increase in fluid heat can be explained by the random or accidental mobility of particles, as this increases the friction force between them. Figure 7, the effect of magnetic parameter is shown in temperature profile. The temperature distribution's behavior in connection the magnetic parameter is described. It is evident that when the magnetic parameter increases, the temperature rises as well. The temperature rises as a result of increased fluid-flow resistance caused by physical increases in magnetic properties. The impact of temperature on the thermophoresis parameter is demonstrated in fig. 8, which also shows how temperature influences the

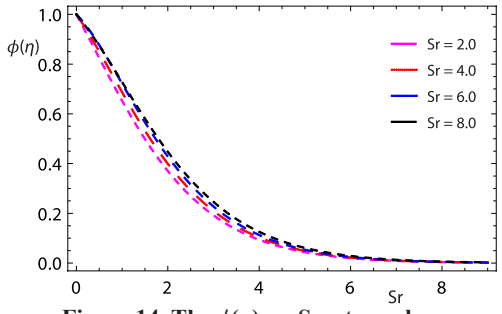

Figure 14. The $\phi(\eta)$ *vs.* Soret number

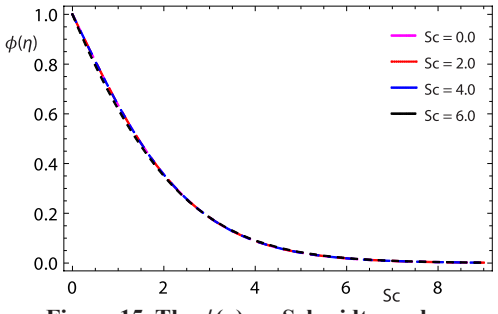

Figure 15. The $\phi(\eta)$ *vs.* Schmidt number

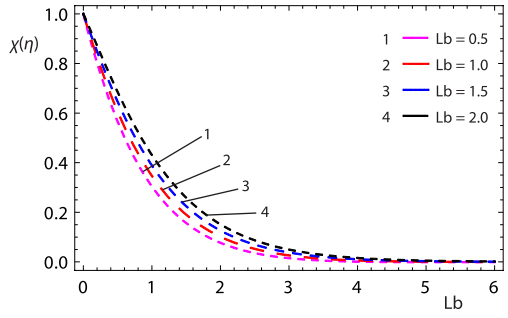

Figure 16. The $\chi(\eta)$ *vs.* Lewis number

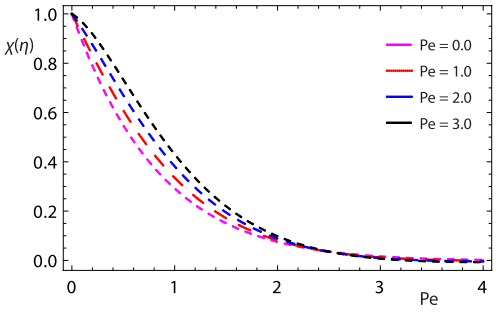

Figure 17. The $\chi(\eta)$ *vs.* Peclet number

thermophoresis parameter. The temperature obviously increases with increasing, *Nt*. As seen in fig. 8, the thermophoresis factor, *Nt*, enhances the flow of nanoparticles from the ambient liquid's warm surface, producing more heat near the border sheet. The impact of the Dufour number on the temperature profile is shown in fig. 9. A rise in temperature is observed as the Dufour number increases. A mixture's overall temperature rises when the Dufour number is large because of the substantial heat produced by the diffusion of various species within it. The relationship between the radiation parameter and the temperature profile is depicted in fig. 10, where it increases in tandem with the radiation parameter. Thenanofluids conduction qualities are enhanced by the heat radiation effect. This occurs because the thermal boundary-layer will become thicker due to increased heat generation. For conduction, a dominant effect is demonstrated. Heat released through radiation causes the system's temperature to rise. The impact of the Brinkman number on the temperature profile is seen in fig. 11. With a higher Brinkman number, the temperature profile rises noticeably, suggesting that the fluids improved ability to produce heat through viscous dissipation causes the temperature to rise more noticeably as Brinkman number increases. The impact of the Brownian motion parameter on the microorganism profile is seen in fig. 12, boost using the Brownian motion parameter tends to reduce the concentration of a microorganism profile. Brownian motion's random movement essentially disperses the microorganisms more uniformly throughout the medium by upsetting any established pattern or concentration gradient within the population. The effect of the thermophoresis parameter on the concentration profile is seen in fig. 13, the concentration profile increases as the thermophoretic parameter, *Nt*, increases. This indicates that too many nanoparticles leave the hot surface, increasing the volume fraction distribution. Figure 14 illustrates how the concentration profile is affected by the Soret number. It displays what happens when the concentration of the Soret number is increased. In this instance, the nanoparticle concentration increases

in tandem with the Soret number. The concentration distribution within the fluid is improved because a higher Soret number indicates a greater link between temperature gradients and mass diffusion which results in a stronger movement of solute particles due to temperature differences. The effect of the Schmidt parameter on the concentration profile is illustrated in fig. 15, which indicates that the volume percentage of nanoparticles decreases as the Schmidt number increases. This is so because the Schmidt number represents the ratio of momentum to mass diffusivity. Consequently, at high Schmidt number values, mass diffusivity falls, requiring a drop in φ. Figure 16 illustrates how the Lewis number affects the profile of microorganisms. In this case, when Lewis number rises, the microbe field grows. Because it suggests a slower rate of mass diffusion than heat transmission, which increases the concentration of microorganisms in the fluid. The effect of Peclet number in microorganisms profile is shown in fig. 17. Which illustrates how the Peclet number affects $\chi(\eta)$. Convective flow becomes more prevalent as the Peclet number rises, causing the fluid to move more quickly and, consequently, a smaller concentration of microorganisms in a particular location.

Conclusions

The flow of bioconvection in Walter-B nanomaterials under the influence of activation energy is the subject of this article. The properties of heat transfer are addressed by thermal radiation. The bvp4c approach is used to solve the modeled equations. The results are given as follows.

- The velocity decreases as the magnetic and viscoelastic properties rise.
- The temperature rises as the radiation parameter , Brownian motion parameter, Dufour number, and Magnetic parameter rise.
- While the thermophoresis parameter increases, concentration increases, but it decreases while the Brownian motion parameter increases.
- As the bioconvection Lewis number and Peclet number rise, so does the field of microorganisms.
- In the future, this study can be extended to incorporate a two-phase nanofluid model. Hybrid nanomaterial-related challenges can also be attempted. In addition slip boundary conditions, other convective heat and mass conditions can be studied.

Nomenclature

B_0 – magnetic field strength
Br – Brinkman number
C – concentration of nanoparticles
C_m – nanoparticles concentration at surface
c_p – heat capacity
D_B – Brownian motion coefficient
D_m – microorganisms diffusion coefficient
D_T – thermophoretic diffusion coefficient
Du – Dufour number
E – activation energy
k – thermal conductivity
M – magnetic parameter
Me – melting variable
N – microorganisms concentration
N_w – microorganisms surface concentration
N_∞ – ambient microorganisms concentration
Nb – Brownian motion parameter
Nt – thermophorosis parameter
Pe – peclet number
Pr – Prantdl number
Rd – radiation parameter
Sc – Schmidt number
Sr – Soret number
T – temperature
T_m – surfacetemperature
W_c – swimming cell speed

Greek symbols

δ_0 – temperature difference number
λ – latent heat
μ – dynamic viscosity
ν – kinematic viscosity
ρ – fluid density
σ – Stephan-Boltzmann constant
Ω – microorganisms concentration difference

References

[1] Walter, K. J., Non-Newtonian Effects in Some Elastic-Viscous Liquids Whose Behaviour at Small Rates of Shear Is Characterized by a General Linear Equation of State, *The Quarterly Journal of Mechanics and Applied Mathematics*, *15* (1962), 1, pp. 63-76
[2] Nandeppanavar, M. M., *et al*., Heat Transfer in a Walter's Liquid B Fluid over an Impermeable Stretching Sheet with Non-Uniform Heat Source/Sink and Elastic Deformation, Communication in Non-linear Science and Numerical Simulation, *15* (2010), 7, pp. 1791-1802
[3] Choi, S. U. S., Eastman, J. A., Enhancing Thermal Conductivity of Fluids with Nanopartiles, No. ANL/MSD/CP-84938;CONF-951135-29, Argonne National Lab. (ANL), Argonne, Ill., USA, 1995
[4] Buongiorno, J., Convective Transport in Nanofluids, *ASME J. of Heat and Mass Transfer*, *128* (2006), 3, pp. 240-250
[5] Hayat, T., *et al*., Radiation Effectson the Mixed Convection flow Induced by an Inclined Stretching Cylinder with Non-Uniform Heat Source/Sink, *PLoS One*, *12* (2017), 4, e0175584
[6] Asghar, A., The 2-D Magnetized Mixed Convection Hybrid Nanofluid over a Vertical Exponentially Shrinking Sheet by Thermal Radiation, *Joul Heating, Velocity and Thermal Slip Condition*, *J. Adv. Fluid Mech.Therm. Sci*., *95* (2022), 2, pp. 159-179
[7] Nadeem, S., *et al*., Inspection of Hybrid Based Nanofluid-Flow over a Curved Surface, *Computer Methods and Programs in Biomedicine*, *189* (2020), 105193
[8] Eshgarf, H., *et al*., A Review of Multi-Phase and Single-Phase Models in the Numerical Simulation of Nanofluid-Flow in Heat Exchangers, *Engineering Analysis with Boundry Elements*, *146* (2023), Jan., pp. 910-927
[9] Ali, K., *et al.*, Thermo-Fluidic Transport Process in Magnetohydrodynamic Couette Channel Containing Hybrid Nanofluid, *Partial Differential Equations in Applied Mathematics*, *7* (2023), 100468
[10] Azam, M., *et al*., The 3-D Convective Flow Sutterby Nanofluid with Activation Energy, *Case Studies in Thermal Engineering*, *50* (2023), 103446
[11] Hussain, M., Sheremet, M., Convection Analysis of the Radiative Nanofluid-Flow through Porous Media over a Stretching Surface with Inclined Magnetic Field, *International Communication in Heat and Mass Transfer*, *140* (2023), 106559
[12] Acharya, N., Kalidas, D., The 3-D Rotating Flow of Cu-Al_20_3/Kerosene Oil Hybrid Nanofluid in Presence of Activation Energy and Thermal Radiation, Numerical Heat Transfer – Part A, *Applications*, *84* (2023), 6, pp. 586-603
[13] Sharma, B. K., *et al*., Bayesianregularization Networks for Micropolar Ternary Hybrid Nanofluid-Flow of Blood with Homogenous and Heterogenous Reaction: Entropy Generation Optimization, *Alexandria Engineering Journal*, *77* (2023), Aug., pp. 127-148
[14] Moatimid, G. M., *et al.*, Heat and Mass Flux through a Reiner-Rivlin Nanofluid-Flow Past a Spinning Stretching Disc: Cattaneo-Christov Model, *Scientific Reports*, *12* (2022), 1, 14468
[15] Turkyilmazoglu, M., Condensation of Laminar Film over Curved Vertical Walls Using Single and Two-Phase Nanofluid Models, *European Journal of Mechanics-B/Fluids*, *65* (2017), Sept.-Oct., pp. 184-191
[16] Muhammad, T., et al., Significance off Non-Linear Thermal Radiation in 3D Eyring-Powell Nanofluid-Flow with Arrhenius Activation Energy, *Journal of Thermal Analysis and Calorimetry*, *143* (2021), 1, pp. 929-944
[17] Awan, S. E., *et al*., Numerical Treatments to Analyze the Non-Linear Radiative Heat Transfer in MHD Nanofluid-Flow with Solar Energy, *Arabian Journal For Science and Engineering*, *45* (2020), May, pp. 4975-499
[18] Sheikholeslami, M., *et al*., Numerical Simulation of MHD Nanofluid-Flow and Heat Transfer Considering Viscous Dissipation, *International Journal of Heat and MassTransfer*, *79* (2014), Dec., pp. 212-222
[19] Maleki, H., *et al*., Heat Transfer and Fluid-Flow of Pseudo-Plastic Nanofluid over a Moving Permeable Plate with Viscous Dissipation and Heat Absorption/Generation, *Journal of Thermal Analysis and Calorimetry*, *135* (2019), 3, pp. 1643-1654
[20] Saleem, S., *et al*., An Optimal Analysis of Radiated Nanomaterial Flow with Viscous Dissipation and Heat Source, *Microsystem Technologies*, *25* (2019), June, pp. 683-689
[21] Ganga, B., *et al.*, The MHD Radiative Boundry Layer Flow of Nanofluid Past a Vertical Plate with Internal Heat Generation/Absorption, Viscous and Ohmic Dissipation Effects, *Journal of the Nigerian Mathematical Society*, *34* (2015), 2, pp. 181-194
[22] Crane, L. J., Flow Past a Stretching Plate, *Zeitschrift fur angewandte Mathematik and physik ZAMP*, *21* (1970), July, pp. 645-647

[23] Elbashbeshy, E. M. A., Bazid, M. A. A., Heat Transferover an Unsteady Stretching Surface, *Heat and Mass Transfer*, *41* (2004), 1, pp. 1-4
[24] Shridan, S., *et al*., Similarity Solutions for the Unsteady Boundry Layer Flow and Heat Transfer Due to a Stretching Sheet, *Applied Mechanics and Engineering*, *11* (2006), 3, 647
[25] Tsai, R., *et al*., Flow and Heat Transfer over an Unsteady Stretching Surface with Non-Uniform Heat Sourc, *International Communication in Heat and Mass Transfer*, *35* (2008), 10, pp. 1340-1343
[26] Ishaq, A., *et al*., Heat Transfer over an Unsteady Stretching Permeable Surface with Prescribed Wall Temperature, Non-Liner Analysis, *Real world Applications*, *10* (2009), 5, pp. 2909-2913
[27] Hayat, T., Awais, M., Simultaneous Sffects of Heat and Mass Transfer on Time-Dependent Flow over a Stretching Surface, *International Journal for Numerical Methods in Fluid*, *67* (2010), 11, pp. 1341-1357
[28] Bhattacharyya, K., *et al*., Slip Effects on an Unsteady Boundary-Layer Stagnation-Point Flow and Heat Transfer Towards a Stretching Sheet, *Chinese Physics Letter*, *28* (2011), 9, 094702
[29] Hayat, T., *et al*., Unsteadyb 3-D flow of Couple Stress Fluid over a Stretching Surface with Chemical Reaction, Non-Linear Analysis, *Modelling and Control*, *17* (2012), 1, pp. 47-59
[30] Rashid, M., *et al*., Magnetohydrodynamic Flow of Maxwell Nanofluid with Binary Chemical Reaction and Arrhenius Activation Energy, *Applied Nanoscience*, *10* (2020), Sept., pp. 2951-2963
[31] Tayebi, T., Chamkha, A. J., Magnetohydrodynamic Natural-Convection Heat Transfer of Hybrid Nanofluid in a Square Enclosure in the Presence of a Wavy Circular Conductive Cylinder, *Journal of Thermal Science and Engineering Applications*, *12* (2020), 3, 031009
[32] Hayat, T., *et al.*, Influence of Arrhenious Activation Energy in MHD Flowof Third Grade Nanofluid over a Non-Linear Stretching Surface with Convective Heat and Mass Condition, *Physica A: Statiscal Mechanics and its Application*, *549* (2020), 124006
[33] Dawar, A., *et al*., Mathematical Modelling and Study of MHD Flow of Williamson Nanofluid over a Non-Linear Stretching Plate with Activation Energy, *Heat Transfer*, *50* (2021), 3, pp. 2558-2570
[34] Hayat, T., *et al*., Effects of Binary Chemical Reaction and Arrhenious Activation Energy in Darcy-Forchhiemer 3-D Flow of Nanofluid Subject to Rotating Frame, *Journal of Thermal Analysis and Calorimetry*, *136* (2019), Oct., pp. 1769-1779
[35] Khan, W. A., *et al*., Consequences of Activation Energy and Binary Chemical Reaction for 3-D Flow of Cross-Nanofluid With Radiative Heat Transfer, *Journal of the Brazilian Society of Mechanical Sciences and Engineering*, *41* (2019), Nov., pp. 1-13
[36] Aziz, A., *et al.*, Free Convection Boundry Layer Flow Past a Horizontal Flat Plate Embedded in Porous Medium Filled by Nanofluid Containing Gyrotactic Microorganisms, *International Journal of Thermal Sciences*, *56* (2012), June, pp. 48-57
[37] Shaw, S., *et al.*, Magnetic Field and Viscous Dissipation Effect on Bioconvection in a Permeable Sphere Embeddedin a Porous Medium with a Nanofluid Containing Gyrotactic Microorganisms, *Heat Transfer-Asian Reseach*, *47* (2018), 5, pp. 718-734
[38] Acharya, N., *et al*., Framing the Effects of Solar Radiation on Magneto-Hydrodynamics Bioconvection Nanofluid-Flow in Presence of Gyrotactic Microorganism, *Journal of Molecular Liquids*, *222* (2016), Oct., pp. 28-37
[39] Khan, W. A., *et al.*, The MHD Boundry Layer Flow of a Nanofluid Containing Gyrotactic Microorganisms Past A Vertical Plate with Navier Slip, *International Journal of Heat and Mass Transfer*, *74* (2014), July, pp. 285-291
[40] Kuznetsov, A. V., The Onset of Nanofluid Bioconvection in a Suspension Containing Both Nanoparticles and Gyrotactic Microorganisms, *International Communications in Heat and Mass Transfer*, *37* (2010), 10, pp. 1421-1425
[41] Mabood, F., *et al.*, The Cu-Al_20_3-H_2O Hybrid Nanofluid-Flow with Melting Heat Transfer, Irreversibility analysis and Non-Linear Thermal Radiation, *Journal of Thermal Analysis and Calorimetry*, *143* (2021), 2, pp. 973-984

Paper submitted: February 2, 2025
Paper revised: May 6, 2025
Paper accepted: July 20, 2025